Guided Organization of λ-DNA into Microring Arrays from Liquid Capillary Bridges

*Myunghwan Byun, Wei Han, Bo Li, Suck Won Hong, Jin Woo Cho, Qingze Zou, and Zhiqun Lin**

A drying droplet on a solid surface (i.e., unbound solution) often leads to the formation of irregular structures, including coffee rings,[1] fingering instabilities,[2] and polygonal networks,[3] owing to the capillary flow induced by nonuniform evaporation flux or temperature-gradient-induced Marangoni convection. Hence, the ability to precisely control the capillary flow and convective flux in drying-mediated self-assembly to create spatially well-defined surface structures has received considerable attention. To date, a few elegant studies have demonstrated intriguing means based on the controlled evaporation in confined geometries (i.e., bound solution) to delicately tailor the evaporative self-organization process, thereby yielding highly ordered structures.[4–23] For example, by rationally designing the upper curved surface in curve-on-flat geometries to accommodate different shapes, a wide range of complex surface patterns with unprecedented regularity were readily produced during the course of solvent evaporation by controlled, repetitive pinning–depinning cycles of the three-phase contact line of the droplet constrained in curve-on-flat geometries.[24] Recently, chemically patterned surface-[25–27] and stamp-assisted deposition methods[28–35] have been exploited for evaporative self-assembly of nonvolatile solutes (e.g., nanoparticles and biomolecules). The use of patterned surfaces or polydimethylsiloxane (PDMS) stamps minimizes uncontrolled droplet shape and possible structural instabilities that may otherwise result in a lack of control over the local dewetting dynamics, and thus produces highly regular surface structures. In a typical capillary-force-induced micromolding process, a micropatterned PDMS mold is in contact with a lower stationary substrate where an evaporating droplet is trapped, covering the lower hydrophobic surface and filling up the space between adjacent PDMS patterns by either one of two capillary motions: the upward capillary rising induced by wetting between the nonpolar solvent and the hydrophobic surface of the PDMS mold,[36,37] or the downward capillary depression induced by dewetting between the polar solvent and the PDMS mold.[38] The former capillary motion has been extensively studied and proven to be more successful.[36,37] In contrast, the latter (i.e., the polar solvent/hydrophobic PDMS system, which is recognized as edge-transfer lithography[38]) has rarely been utilized due to difficult control over the dewetting of the solution. The capillary action of the solution constrained in the confined geometry can be significantly influenced by the shape and curvature of the molds, thereby providing new opportunities for controlling the local dewetting dynamics to form ordered structures.[24]

Herein, we demonstrate a facile route to creating λ-DNA microring arrays via dewetting-induced self-assembly guided by liquid capillary microbridges. These microscopic liquid bridges were yielded by constraining a drop of λ-DNA aqueous solution in the space produced by placing the PDMS hemispherical microlens arrays in contact with the lower stationary substrate. This simple yet robust approach can be easily extended to form arrays of a diverse set of nonvolatile solutes, such as proteins, peptides, antibodies, carbon nanotubes, and nanoparticles.

The PDMS hemispherical arrays were replicated from a metallic Ni master mold fabricated by the combination of a thermal reflowing of photoresist (PR) patterns[39] and electrodeposition,[40] as illustrated in **Figure 1**. Briefly, the circular PR arrays produced by photolithography were transformed into hemispherical microlens arrays due to surface tension via the thermal reflowing process.[39] A thin layer of Au/Cr was deposited on the arrays by thermal evaporation, followed by the electroplating of Ni. The Ni electrodeposit was then released from the Si substrate. Finally, the PDMS microlens replica was obtained after the PDMS casting, curing, and removal from the Ni mold (Figure 1 and Experimental Section). Representative optical micrographs of PR arrays before and after the thermal reflowing,

M. Byun, W. Han, B. Li, S. W. Hong, Prof. Z. Q. Lin
Department of Materials Science and Engineering
Iowa State University
Ames, IA 50011, USA
E-mail: zqlin@iastate.edu
W. Han, B. Li, Prof. Z. Q. Lin
School of Materials Science and Engineering
Georgia Institute of Technology
Atlanta, GA 30332, USA
Dr. J. W. Cho
Green Energy Research Center
Korea Electronics Technology Institute
Gyeonggi 463-816, South Korea
Prof. Q. Zou
Department of Mechanical and Aerospace Engineering
Rutgers, the State University of New Jersey
Piscataway, NJ 08854, USA

DOI: 10.1002/smll.201100186

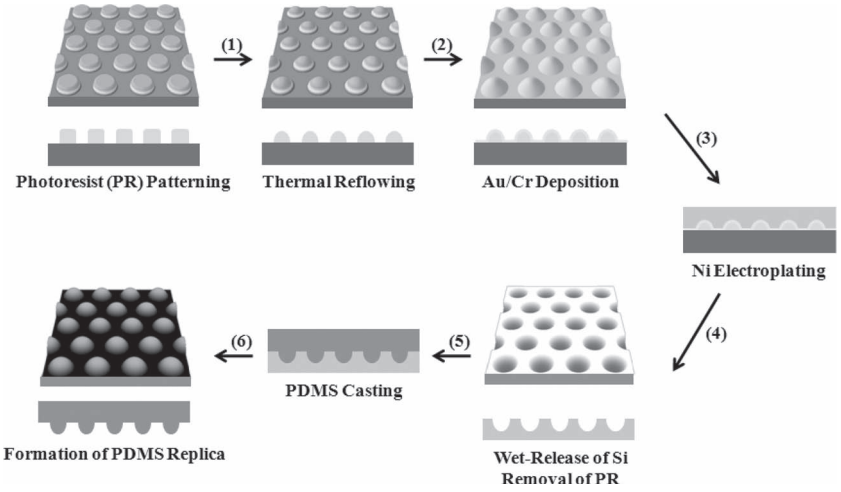

Figure 1. Schematic illustration of the preparation of the PDMS hemispherical microlens arrays. 1) Circular PR arrays formed by photolithography were transformed into hemispherical microlenses via a thermal reflowing process. 2) Thermal evaporation of Au/Cr. 3) Electroplating of Ni onto the hemispherical PR arrays. 4) Wet-release of Ni electrodeposit from the Si wafer. 5) PDMS casting. 6) Formation of PDMS replica.

hemispherical arrays with Ni electroplated, and a PDMS replica are shown in Figure S1 (Supporting Information).

DNA is a promising construction material for producing well-defined micro- or nanostructures for practical applications in electronic, magnetic, photonic, optical, and sensory materials and devices.[41–45] The ability to place a large number of DNA molecules in a well-controlled arrangement is key to integrating them into these functional devices. In this regard, we capitalized on the newly obtained PDMS replica to produce regular fluorescent dye, YOYO-1-labeled λ-DNA microring arrays over large surface areas by evaporative self-assembly via controlled dewetting of the λ-DNA solution in microscopic liquid capillary bridges, as depicted in **Figure 2** (*see also* Experimental Section). First, a drop of λ-DNA aqueous solution (5 μL, 5 μg mL^{-1}) was loaded on the poly(methyl methacrylate) (PMMA)-coated Si substrate, and then the PDMS replica was placed on top of the droplet (Figure 2a). The λ-DNA solution was spontaneously spread over the entire surface of the PDMS replica and occupied the space between neighboring hemispheres (first panel in Figure 2b). As the evaporation progressed, the interplay of capillary movement and hydrophobic repulsion-induced dewetting originating from the unfavorable interaction between water and hydrophobic PMMA and PDMS led the solution to form menisci in the microgap between the hemispherical microlens and the PMMA-coated substrate (second panel in Figure 2b). After complete water evaporation, arrays of well-ordered microscopic λ-DNA rings over large surface areas were obtained (third panel in Figure 2b and Figure 2c). The diameter of the λ-DNA microrings can be readily tailored by the proper choice of a PDMS replica of different size. Representative fluorescence micrographs of microring arrays of different diameters are shown in **Figure 3**. The λ-DNA was labeled with YOYO-1, which emitted green fluorescence (coverted into gray scale in Figure 3). The present study opens up a simple yet robust route to fabricating patterned DNA arrays via the synergy of surface dewetting and evaporative deposition. We note that ringlike structures composed of other materials have been demonstrated on some occasions.[46–50]

To scrutinize the surface morphologies of λ-DNA microrings and their dimensions, and more importantly to better understand their formation mechanism due to the competition between the capillary rising and capillary depression during the evaporative self-assembly of λ-DNA microfluid in the microgap, atomic force microscopy (AFM) measurements were performed (**Figure 4** and Figure S2, Supporting Information). The lateral size (i.e., diameter, D_{PDMS}) of the PDMS microlenses used in the study varied from 95 μm (largest; #1) to 15 μm (smallest; #9) with an interval of 10 μm, while the height of the lenses was constant at 5 μm (Figure S1). The diameter of λ-DNA rings was correlated with the size of PDMS microlens used. The average height of λ-DNA rings was 79.8 ± 13 nm (Figure S2). The height variation is presumably due to the lack of precise control over topological changes of the PR patterns during the thermal

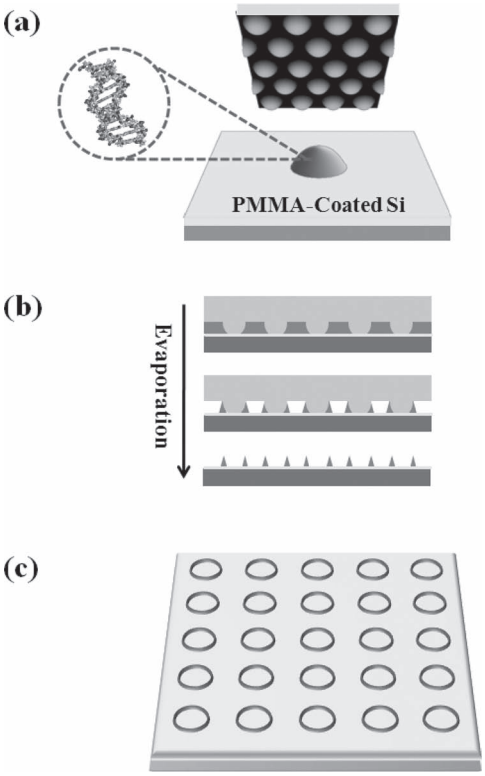

Figure 2. Schematic representation of λ-DNA microring arrays formed by controlled evaporative self-assembly in liquid capillary bridges. a) A drop of λ-DNA solution (5 μL) was loaded on the PMMA-coated Si substrate, followed by placing the PDMS microlenses against the droplet. b) 2D cross-sectional view of the deposition of λ-DNA as water evaporated. c) λ-DNA microring arrays formed on a PMMA-coated Si substrate (3D view).

small NANO MICRO

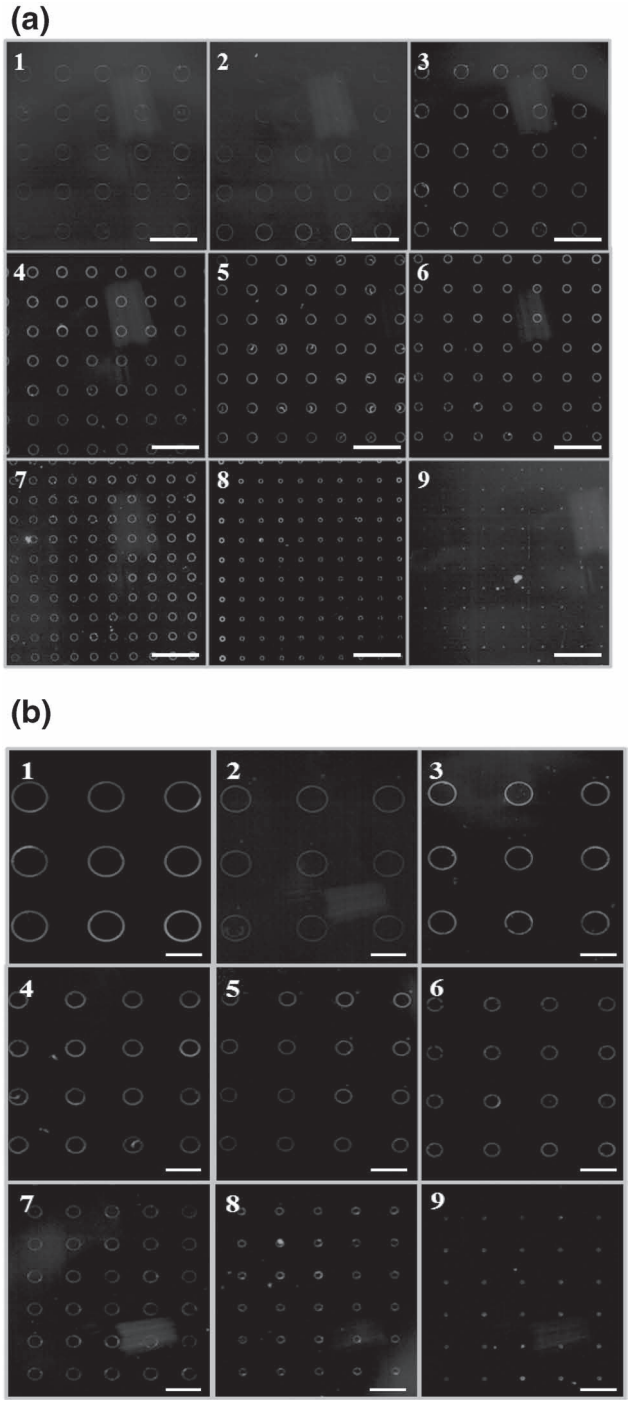

Figure 3. Representative fluorescence micrographs of λ-DNA microring arrays (converted into gray scale). a) Fluorescence images of λ-DNA microrings with a wide variation in diameter formed on the hydrophobic PMMA surface over large areas were taken after the removal of the PDMS microlenses; scale bar: 200 μm. b) The corresponding close-up images; scale bar: 100 μm.

reflowing process, which directly affected the PDMS replication process. The average width of the λ-DNA rings was 1.3 ± 0.3 μm (Figure S3).

It is noteworthy that the diameter of isolated microrings appeared to be smaller than the diameter of the PDMS microlenses used (i.e., D_{DNA} = 89.7 μm vs. D_{PDMS} = 95 μm from replica #1; D_{DNA} = 78.2 μm vs. D_{PDMS} = 85 μm from #2; D_{DNA} = 69.4 μm vs. D_{PDMS} = 75 μm from #3; D_{DNA} = 57.7 μm vs. D_{PDMS} = 65 μm from #4; D_{DNA} = 48.1 μm vs. D_{PDMS} = 55 μm from #5; D_{DNA} = 38.3 μm vs. D_{PDMS} = 45 μm from #6; D_{DNA} = 29.8 μm vs. D_{PDMS} = 35 μm from #7; D_{DNA} = 19.3 μm vs. D_{PDMS} = 25 μm from #8; and D_{DNA} = 7.7 μm vs. D_{PDMS} = 15 μm from # 9; Figure 4). This suggested that the confined hydrophilic λ-DNA solution slightly receded toward the contact center of the PDMS microlens and PMMA-coated substrate due to different capillary interaction at the hydrophobic PDMS/DNA solution interface and at the hydrophobic PMMA/DNA solution interface, forming λ-DNA ringlike deposits conforming to the shape of the upper microlens (**Figure 5**).

The capillary action can be further understood by considering the different capillary movement of the meniscus in microscopic liquid bridges. As the gravity effect is negligible, the length of capillary to be filled is determined by the surface tension, the solution viscosity,[30,31,37] the contact angle of the λ-DNA solution, and the size of capillary, and is given by:[30,31,37]

$$Z = \left(\frac{t R\gamma |\cos\theta|}{2\eta}\right)^{1/2} \quad (1)$$

where Z is the length of the capillary movement (i.e., Z_{PDMS} on the PDMS surface, and Z_{PMMA} on the PMMA surface), t is the time for filling up the microgap between the upper PDMS microlens and the lower PMMA-coated Si surface ($t \approx 5$ s according to experimental observation), R is the hydraulic radius calculated based on Pythagoras' theorem using the capillary height at the PDMS/PMMA interface and the contact angle (i.e., the ratio of the liquid volume in the capillary bridge to the area of the solid/liquid interface; R_{PDMS}: at the PDMS/λ-DNA solution interface, $R_{PDMS} \approx 9.725$ μm, marked with a dotted blue line in Figure 5b; and R_{PMMA}: at the PMMA/λ-DNA solution interface, $R_{PMMA} \approx 7.364$ μm, marked with a dotted red line in Figure 5b), γ is the surface tension of the λ-DNA solution ($\gamma \approx 72$ dyn cm^{-1}),[51] θ is the advancing contact angle of the λ-DNA solution on the solid surface (i.e., θ_{PDMS}: advancing contact angle of the λ-DNA solution on the PDMS surface, $\theta_{PDMS} \approx 105°$;[30] and θ_{PMMA}: on the PMMA surface, $\theta_{PMMA} \approx 70°$[30]), and η is the viscosity of the solution ($\eta \approx 8.9 \times 10^{-4}$ dyn·s cm^{-2}, the dynamic viscosity of water).[51]

The contact angle of the λ-DNA solution is approximately 105° on the upper PDMS surface, which reflects a capillary depression (i.e., $\cos\theta_{PDMS} < 0$; $Z_{PDMS} < 0$ representing a downward capillary depression). In contrast, on the PMMA surface, the λ-DNA solution has the contact angle of 70° (i.e., $\cos\theta_{PMMA} > 0$; $Z_{PMMA} > 0$ reflecting an upward capillary rising). Thus, the net length of the capillary movement on two different interfaces is $Z_{net} = (Z_{PDMS} + Z_{PMMA}) = 4.06$ μm calculated based on Equation (1), thus indicating an inward retraction of the meniscus (i.e., toward the PDMS/PMMA contact center), which is comparable to (or only slightly higher than) the value obtained experimentally, that is, $(D_{PDMS} - D_{DNA})/2 = 3.15 \pm 0.5$ μm, where D_{PDMS} and D_{DNA} are the diameters of a PDMS microlens and a λ-DNA ring, respectively (Figure 5a). This explained the

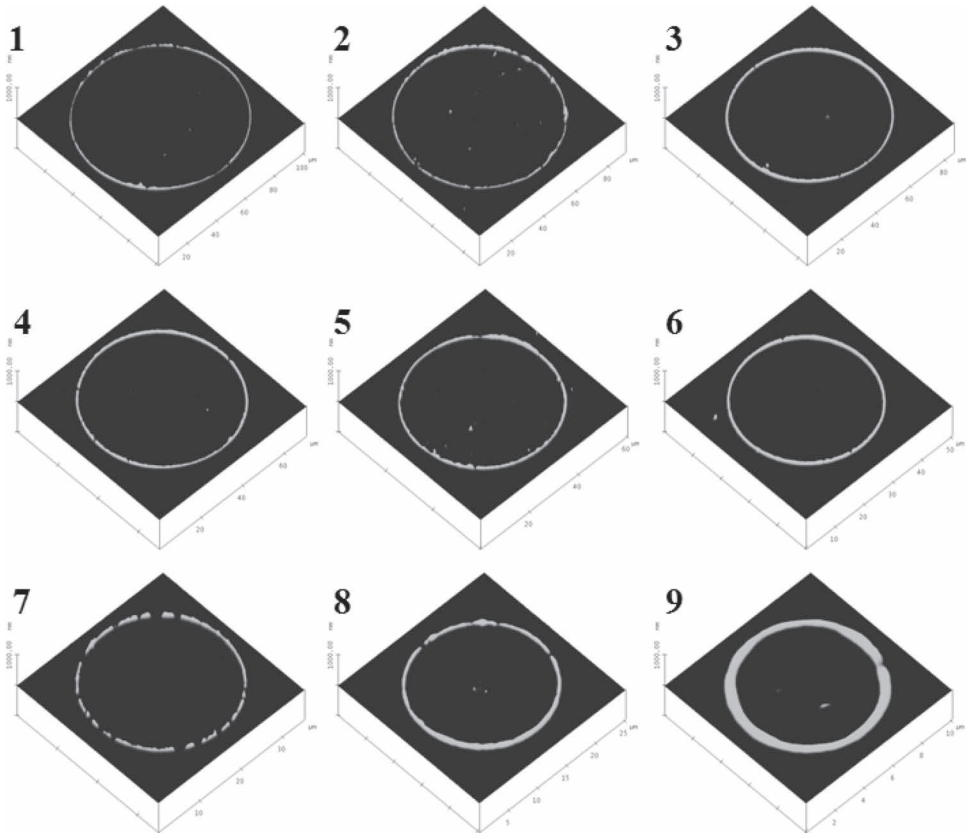

Figure 4. Representative 3D AFM height images of individual λ-DNA microrings. The scan sizes were 100 × 100 μm^2 for mold #1, 90 × 90 μm^2 for #2, 85 × 85 μm^2 for #3, 70 × 70 μm^2 for #4, 60 × 60 μm^2 for #5, 50 × 50 μm^2 for #6, 35 × 35 μm^2 for #7, 25 × 25 μm^2 for #8, and 10 × 10 μm^2 for #9.

formation of λ-DNA rings with diameter smaller than that of the PDMS microlenses during water evaporation (Figure 5c).

The resulting λ-DNA microring was composed of a number of DNA nanofibers (i.e., forming DNA bundles, Figure S3) rather than the single nanowire observed in stretched DNA (i.e., molecular combing of DNA).[52] This is not surprising because during the evaporation process λ-DNA molecules were densely concentrated at the edge of the three-phase contact line. They aggregated and adopted the coil conformation as the evaporation progressed.[53] Moreover, in the present study, no external force was applied to stretch λ-DNA, and the inward capillary flow as a result of water evaporation was not strong enough to align the λ-DNA molecules.

In summary, λ-DNA microring arrays were successfully fabricated through controlled evaporative self-assembly in liquid capillary bridges. The size of the microrings can be readily controlled by the proper choice of the PDMS microlens replica. This viable approach opens up a new avenue to utilize controlled evaporation as an alternative to conventional lithography techniques for creating patterned biomolecular arrays in a simple and cost-effective manner. By capitalizing on this facile approach, a wide variety of biomaterials can be easily spatially organized into well-ordered arrays, which may promise potential applications in functional scaffolds for cell and tissue growth, biosensors, etc.

Experimental Section

Preparation of Nickel Master Mold with Concave Microhemispheres: As illustrated in Figure 1, to fabricate Ni master molds with different sizes of convex microhemispheres, a positive PR (AZ9260) was first spin-coated and soft-baked at 110 °C for 60 s to enhance the adhesion between the PR and Si. The thickness of the PR was 5 μm. The PR-deposited Si wafer was exposed on an I-line stepper to a dose of 225 mJ cm^{-2}. After development with MIS300, cylindrical micropatterns were obtained. Subsequently, thermal reflowing at 120 °C for 5 min transformed circular disk-shaped PR patterns into hemispherical microlens arrays (Figure S1a, Supporting Information; after thermal reflowing, bright dots in the center of the microlens were observed due to light reflection originating from the curved microlens surface[39]). To coat a conductive layer on the patterned surface, chromium and gold were vapor-deposited. The thickness of these two layers was 50 and 150 nm, respectively. Ni electroplating was conducted in a nickel sulfite electrolyte with dc current density of 4 A dm^{-2}. The temperature and pH of the electrolyte were kept at 55 °C and 4.0 ± 0.1, respectively.[40] The electrodeposition of Ni took 50 min at the deposition rate of 1 μm min^{-1}, yielding a final thickness of 50 μm. After electroplating, the bottom of the Si wafer was wet-released with tetramethylammonium hydroxide (TMAH) solution (20 wt.% at 80 °C; etching rate ≈ 0.6 μm min^{-1}). Subsequently, PR residue and conductive layers were removed by acetone and chemical etchants.

NANO MICRO small

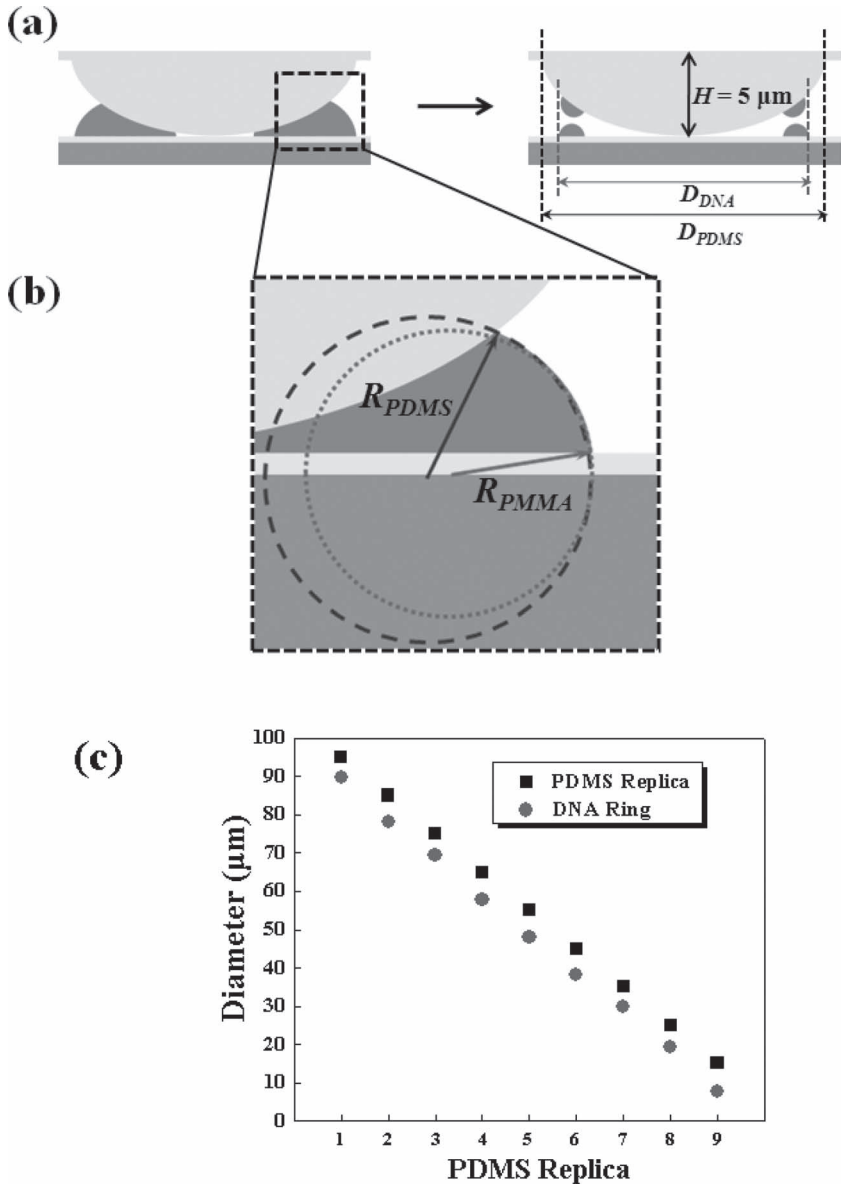

Figure 5. a) Schematic illustration of the formation mechanism of a λ-DNA microring in a liquid capillary bridge. Left: λ-DNA solution is trapped in the microgap between the upper PDMS microlens surface and the lower PMMA-coated surface. In the λ-DNA solution capillary bridge, DNA molecules moved inward due to the interplay of capillary movement and hydrophobic repulsion-induced dewetting (i.e., unfavorable interaction between PDMS and λ-DNA solution as well as between PMMA and λ-DNA solution). Right: after the evaporation was completed, a λ-DNA microring with smaller diameter than that of the PDMS microlens was produced. b) Schematic illustration of the different hydraulic radius formed at two interfaces (i.e., PDMS/λ-DNA and PMMA/λ-DNA solution interfaces), marked in the left panel of (a). c) The diameter of λ-DNA microrings obtained using differently sized PDMS microlens arrays in comparison with the diameter of the corresponding PDMS microlenses.

Preparation of PDMS Replica with Hemispherical Microlens Arrays: The PDMS microlens arrays were replicated by casting PDMS precursor mixed with 10 wt% curing agent (Sylgard 184, Dow Corning) onto the Ni masters noted above. Prior to casting, the Ni master was treated with a silane agent, tridecafluoro-1,1,2,2-tetrahydrooctyl trichlorosilane. The cast PDMS precursor was cured at 100 °C for 45 min and then released from the Ni masters (Figure S1b). A PDMS replica of different size was thus obtained (Figure S1c). The replica was cut into small pieces of desired size (2×2 cm^2) prior to usage.

PMMA-Coated Si Substrate: A p-type silicon wafer (100) was first cleaned with a mixture of sulfuric acid and Nonchromix, and then vigorously rinsed with deionized water and blow-dried with N_2. The cleaned Si wafer was cut into small pieces of size 3×3 cm^2. Subsequently, hexamethyldisilazane (HMDS) was spin-coated on the Si substrate at 3000 rpm, followed by coating with PMMA (molecular weight = 534 kg mol^{-1}) in toluene solution (concentration, c = 4 mg mL^{-1}) on the HMDS-coated Si substrate at 2000 rpm. To enhance the adhesion between PMMA and silicon native oxide on Si and to prevent PMMA from dewetting,[54] HMDS was spin-coated prior to the deposition of PMMA. The resulting PMMA-coated Si substrate was annealed at 120 °C for 1 h. After thermal annealing, no dewetted region appeared and the root-mean-square surface roughness was slightly reduced from 1.010 nm (Figure S4; before annealing) to 0.788 nm (Figure S4b; after annealing).

Preparation of λ-DNA Solution: To prepare the DNA solution, λ-DNA (New England Biolabs; 48 502 bp, 500 μg mL^{-1} in 10 mM Tris·HCl/1 mM ethylenediaminetetraacetic acid (EDTA), pH ≈ 8.0), DNase-free TE buffer (Sigma (T9285-100 mL); 100× concentrate, 0.2 μm filtered, 1.0 M Tris·HCl/0.1 M EDTA, pH≈8.0), and a fluorescent YOYO-1 iodide (Invitrogen; 1 mM solution in dimethyl sulfoxide (DMSO), 200 μL) were used as supplied without further purification. The DNase-free TE buffer was first diluted by adding ultrapure water (9.9 mL, deionized and distilled) to TE buffer solution (0.1 mL). Subsequently, this diluted DNase-free buffer solution (10 mM Tris·HCl/1 mM EDTA, pH ≈ 7.5–8.0) was used to prepare λ-DNA solution (5 μg mL^{-1}). For fluorescence labeling of λ-DNAs at a dye/base-pair ratio of 1:2, YOYO-1 iodide (10 μL) was directly taken from the original solution and added to the 5 μg mL^{-1} λ-DNA solution (2.54 mL). All procedures were conducted in the dark to prevent the dyes from bleaching. Finally, a fluorescent λ-DNA solution (2.64 mL, 5 μg mL^{-1}) was yielded.

Construction of Confined Geometry: To implement a confined geometry in which the λ-DNA solution was constrained, an inchworm motor with a step motion of a few hundred micrometers was applied to allow the upper PDMS microlens replica to be in contact with the lower stationary PMMA-coated substrate (Figure 2a). Before contact, a drop of λ-DNA solution (5 μL, 5 μg mL^{-1}) was loaded and trapped within the gap between the PDMS hemispherical microlens array and the PMMA-coated Si substrate (Figure 2b). Finally, the upper PDMS replica was brought into contact with the PMMA-coated Si by the inchworm motor.

Characterization: Optical imaging was performed in the reflection mode under blue light and was also combined with fluorescent light (Olympus BX51). AFM imaging of λ-DNA rings was obtained by using a scanning force microscope in tapping mode (Digital Instruments Dimension 3100). BS-tap300 tips with spring constants ranging from 20 to 75 N m^{-1} were used as scanning probes (Budget Sensors).

Supporting Information

Supporting Information (optical micrographs of PDMS microlens arrays, AFM images of λ-DNA and the corresponding section analysis, and surface roughness analysis of PMMA-coated Si substrates) is available from the Wiley Online Library or from the author.

Acknowledgements

We gratefully acknowledge support from the National Science Foundation (NSF CMMI-0968656).

[1] R. D. Deegan, O. Bakajin, T. F. Dupont, G. Huber, S. R. Nagel, T. A. Witten, *Nature* **1997**, *389*, 827.
[2] E. Pauliac-Vaujour, A. Stannard, C. P. Martin, M. O. Blunt, I. Notingher, P. J. Moriarty, I. Vancea, U. Thiele, *Phys. Rev. Lett.* **2008**, *100*, 176102.
[3] V. X. Nguyen, K. J. Stebe, *Phys. Rev. Lett.* **2002**, *88*, 164501.
[4] M. Abkarian, J. Nunes, H. A. Stone, *J. Am. Chem. Soc.* **2004**, *126*, 5978.
[5] Z. Q. Lin, S. Granick, *J. Am. Chem. Soc.* **2005**, *127*, 2816.
[6] J. Xu, J. F. Xia, S. W. Hong, Z. Q. Lin, F. Qiu, Y. L. Yang, *Phys. Rev. Lett.* **2006**, *96*, 066104.
[7] J. Xu, J. F. Xia, Z. Q. Lin, *Angew. Chem. Int. Ed.* **2007**, *46*, 1860.
[8] H. Yabu, M. Shimomura, *Adv. Funct. Mater.* **2005**, *15*, 575.
[9] M. Byun, R. L. Laskowski, M. He, F. Qiu, M. Jeffries-El, Z. Q. Lin, *Soft Matter* **2009**, *5*, 1583.
[10] S. W. Hong, J. Wang, Z. Q. Lin, *Angew. Chem. Int. Ed.* **2009**, *48*, 8356.
[11] S. W. Hong, J. F. Xia, Z. Q. Lin, *Adv. Mater.* **2007**, *19*, 1413.
[12] M. Byun, N. B. Bowden, Z. Q. Lin, *Nano Lett.* **2010**, *10*, 3111.
[13] M. Byun, W. Han, F. Qiu, N. B. Bowden, Z. Q. Lin, *Small* **2010**, *6*, 2250.
[14] Z. Q. Lin, *J. Polym. Sci., Part B: Polym. Phys.* **2010**, *48*, 2552.
[15] S. W. Hong, S. Giri, V. S. Y. Lin, Z. Q. Lin, *Chem. Mater.* **2006**, *18*, 5164.
[16] S. W. Hong, W. Jeong, H. Ko, M. R. Kessler, V. Tsukruk, Z. Q. Lin, *Adv. Funct. Mater.* **2008**, *18*, 2114
[17] S. W. Hong, J. Xia, M. Byun, Q. Zou, Z. Q. Lin, *Macromolecules* **2007**, *40*, 2831.
[18] S. W. Hong, J. Xu, Z. Q. Lin, *Nano Lett.* **2006**, *6*, 2949.
[19] S. W. Hong, J. Xu, J. Xia, Z. Q. Lin, F. Qiu, Y. L. Yang, *Chem. Mater.* **2005**, *17*, 6223.
[20] M. Byun, S. W. Hong, F. Qiu, Q. Zou, Z. Q. Lin, *Macromolecules* **2008**, *41*, 9312.
[21] M. Byun, S. W. Hong, L. Zhu, Z. Q. Lin, *Langmuir* **2008**, *24*, 3525.
[22] M. Byun, J. Wang, Z. Q. Lin, *J. Phys.: Condens. Matter* **2009**, *21*, 264014.
[23] M. Byun, J. Wang, Z. Q. Lin, *Acta Phys. Chim. Sin.* **2009**, *25*, 1249.
[24] S. W. Hong, M. Byun, Z. Q. Lin, *Angew. Chem. Int. Ed.* **2009**, *48*, 512.
[25] W. L. Cheng,N. Y. Park, M. T. Walter, M. R. Hartman, D. Luo, *Nat. Nanotechnol.* **2008**, *3*, 682.
[26] A. Kumar, G. M. Whitesides, *Science* **1994**, *263*, 60.
[27] R. J. Kershner, L. D. Bozano, C. M. Micheel, A. M. Hung, A. R. Fornof, J. N. Cha, C. T. Rettner, M. Bersani, J. Frommer, P. W. K. Rothemund, G. M. Wallraff, *Nat. Nanotechnol.* **2009**, *4*, 557.
[28] E. Bystrenova, M. Facchini, M. Cavallini, M. G. Cacace, F. Biscarini, *Angew. Chem. Int. Ed.* **2006**, *45*, 4779.
[29] E. Delamarche, A. Bernard, H. Schmid, A. Bietsch, B. Michel, H. Biebuyck, *J. Am. Chem. Soc.* **1998**, *120*, 500.
[30] E. Kim, Y. N. Xia, G. M. Whitesides, *Nature* **1995**, *376*, 581.
[31] E. Kim, Y. N. Xia, G. M. Whitesides, *J. Am. Chem. Soc.* **1996**, *118*, 5722.
[32] B. Messer, J. H. Song, P. D. Yang, *J. Am. Chem. Soc.* **2000**, *122*, 10232.
[33] G. Shi, N. Lu, L. G. Gao, H. B. Xu, B. J. Yang, Y. Li, Y. Wu, L. F. Chi, *Langmuir* **2009**, *25*, 9639.
[34] K. Y. Suh, S. J. Choi, S. J. Baek, T. W. Kim, R. Langer, *Adv. Mater.* **2005**, *17*, 560.
[35] C. M. Bruinink, M. Peter, P. A. Maury, M. De Boer, L. Kuipers, J. Huskens, D. N. Reinhoudt, *Adv. Funct. Mater.* **2006**, *16*, 1555.
[36] Y. S. Kim, K. Y. Suh, H. H. Lee, *Appl. Phys. Lett.* **2001**, *79*, 2285.
[37] K. Y. Suh, Y. S. Kim, H. H. Lee, *Adv. Mater.* **2001**, *13*, 1386.
[38] O. Cherniavskaya, A. Adzic, C. Knutson, B. J. Gross, L. Zang, R. Liu, D. M. Adams, *Langmuir* **2002**, *18*, 7029.
[39] P. Ruther, B. Gerlach, J. Gottert, M. Ilie, J. Mohr, A. Muller, C. Ossmann, *Pure Appl. Opt.* **1997**, *6*, 643.
[40] M. Byun, J. W. Cho, B. S. Han, Y. K. Kim, Y. S. Song, *Jpn. J. Appl. Phys., Part 1* **2006**, *45*, 7084.
[41] E. Braun, Y. Eichen, U. Sivan, G. Ben-Yoseph, *Nature* **1998**, *391*, 775.
[42] H. Yan, S. H. Park, G. Finkelstein, J. H. Reif, T. H. LaBean, *Science* **2003**, *301*, 1882.
[43] E. Winfree, F. R. Liu, L. A. Wenzler, N. C. Seeman, *Nature* **1998**, *394*, 539.
[44] X. D. Su, R. Robelek, Y. J. Wu, G. Y. Wang, W. Knoll, *Anal. Chem.* **2004**, *76*, 489.
[45] S. Tombelli, R. Mascini, L. Braccini, M. Anichini, A. P. F. Turner, *Biosens. Bioelectron.* **2000**, *15*, 363.
[46] W. S. Chang, L. S. Slaughter, B. P. Khanal, P. Manna, E. R. Zubarev, S. Link, *Nano Lett.* **2009**, *9*, 1152.
[47] K. L. Genson, J. Hoffman, J. Teng, E. R. Zubarev, D. Vaknin, V. V. Tsukruk, *Langmuir* **2004**, *20*, 9044.
[48] B. P. Khanal,E. R. Zubarev, *Angew. Chem. Int. Ed.* **2007**, *46*, 2195.
[49] G. Lu, W. Li,J. M. Yao,G. Zhang, B. Yang,J. C. Shen, *Adv. Mater.* **2002**, *14*, 1049.
[50] A. P. H. J. Schenning, F. B. G. Benneker, H. P. M. Geurts, X. Y. Liu, R. J. M. Nolte, *J. Am. Chem. Soc.* **1996**, *118*, 8549.
[51] H. E. Jeong, P. Kim, M. K. Kwak, C. H. Seo, K. Y. Suh, *Small* **2007**, *3*, 778.
[52] X. Michalet, R. Ekong, F. Fougerousse, S. Rousseaux, C. Schurra, N. Hornigold, M. van Slegtenhorst, J. Wolfe, S. Povey, J. S. Beckmann, A. Bensimon, *Science* **1997**, *277*,1518.
[53] M. G. Cacace, E. M. Landau, J. J. Ramsden, *Q. Rev. Biophys.* **1997**, *30*, 241.
[54] M. J. Madou, *Fundamentals of Microfabrication: The Science of Miniaturization*, 2nd ed., CRC Press, Boca Raton, **2002**.

Received: January 27, 2011
Published online: April 26, 2011